

# Grid-based Cyclic Robot Allocation for Object Carrying

Jee Hwan Park<sup>1</sup>, Tamzidul Mina<sup>1</sup> and Byung-Cheol Min<sup>2</sup>

**Abstract**—Object carrying by a multi-robot group of spherical robots is a versatile object transportation strategy compared to the traditional grasping, pushing or caging methods proposed in literature. In this paper we address the fundamental problem of multi-robot allocation for object carrying by a group of spherical robots. A grid-based cyclic robot allocation (GCRA) method for spherical robots is proposed along with specific stability criterion, that designs the grid size parameters and identifies the minimum number of robots required based on the arbitrary shape of a given object for stable omni-directional translation of the object on a planar surface. An analytical proof of the proposed cyclic robot allocation method is shown verifying stability of the transportation process. Experimental results of robot allocation using GCRA for several arbitrary shapes validate the proposed method.

## I. INTRODUCTION

Object transportation using multi-robot systems has been a popular research topic due to its robustness and fault tolerant features. Over the years, significant improvements in individual robot capabilities for object manipulation and coordinating with others in a group have been observed for successful implementation of multi-robot object transportation in the field. As a result, popular methods of object transportation by multi-robot systems have remained confined to grasping [1], pushing [2] and caging [3] strategies.

These strategies have proven to be effective methods for object transportation but still suffer from certain limitations as follows:

- Force applied by individual robots strongly depends on the weight of the object which directly relates to friction during the transportation process.
- Direction of the transportation relies on the formation of multi-robot system which requires real-time coordination of agents.
- Pushing strategies may damage the object being transported or the pushing robot itself due to impact.
- An object must have graspable features when using the grasping strategy.

These limitations can be addressed by a multi-robot system of spherical robots [4] [5] rolling and carrying the object for transportation. The spherical design of the carrying robots allow fast and efficient omni-directional translation without requiring any complex inter-agent coordination as long as the object is supported from underneath. An effective robot

<sup>1</sup>Jee Hwan Park and Tamzidul Mina are with the SMART Lab, Department of Computer and Information Technology, Purdue University, and with the School of Mechanical Engineering, Purdue University, West Lafayette, IN 47907, USA [tmina,park458@purdue.edu](mailto:tmina,park458@purdue.edu)

<sup>2</sup>Byung-Cheol Min is with the SMART Lab, Department of Computer and Information Technology, Purdue University, West Lafayette, IN 47907, USA [minb@purdue.edu](mailto:minb@purdue.edu)

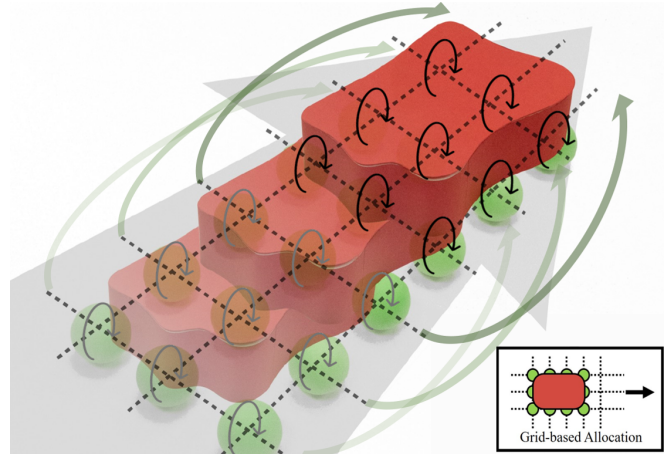


Fig. 1: Object carrying by spherical robots concept illustrating proposed grid-based robot allocation (GCRA). Spherical robots allocated by GCRA roll under the object for object omni-directional translation. Robots at the back losing contact, cycle around to the front to receive object and continue translation in the desired direction.

allocation method can ensure even distribution of object weight on carrying spherical robots to minimize individual effort during the transportation process. Furthermore, the object does not require any special features for pushing or grasping allowing wider applicability.

A fundamental problem for object carrying by a multi-robot group of spherical robots is robot allocation under the object for safe transportation. Robots must coordinate their positions to ensure safe carrying of the object and prevent any individual from experiencing excessive weight of the object. Therefore, as preliminary work we present a Grid-based Cyclic Robot Allocation (GCRA) method in this paper, that designs grid size parameters and the minimum number of robots required based on the arbitrary shape of a given object for stable omni-directional translation on a planar surface. The proposed spherical robot allocation method for object carrying ensures system stability with adequate redundancies in case of individual robot failures.

## II. RELATED WORKS

Object or payload transportation using multi-robot systems has been extensively studied in literature with particular focus on object pushing, grasping or caging strategies. In comparison, very few feasible methodologies have been proposed for object transport by carrying. A recent review on multi-robot object transportation by Tuci *et al.* [6] categorized object carrying methods under grasping strategies since the robots align their forces and sustain the transport

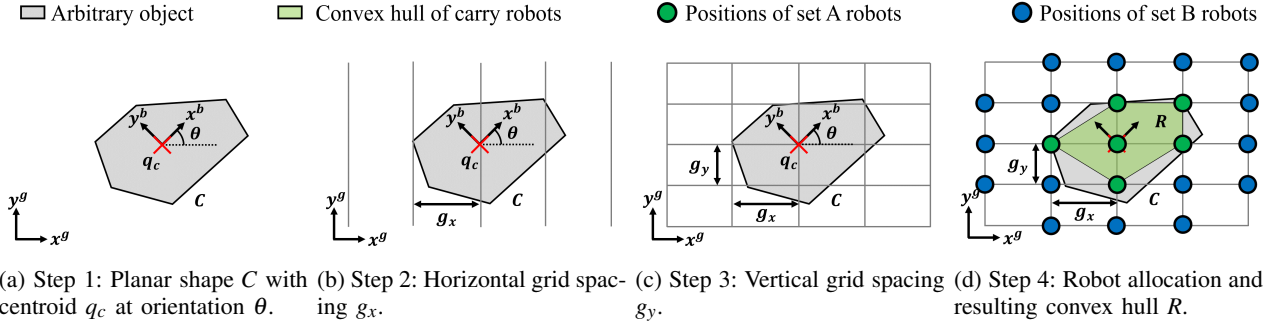


Fig. 2: Steps of grid generation for robot allocation based on the arbitrary planar shape  $C$ . Positions of set A robots under  $C$  are represented with green circles, and position of set B robots around the object are represented with blue circles in (d).

without losing physical contact with the object.

Some of the earliest work on multi-robot object carrying were proposed by Stilwell *et al.* [7] and Johnson *et al.* [8] where a group of ant-like robots transported palletized loads of unknown mass and center of geometry in a distributed system. Coordination between the robots was achieved based on sensing the forces applied on the object by the robots. Similar coordination in object carrying were later implemented in [9] and [10] with a leader-follower approach.

A centralized approach to object carrying by a group of homogeneous robots with manipulator arms was proposed by Hichri *et al.* in [11]. Coordination and determination of optimal locations for robots while carrying the object were determined by a central server with a priori knowledge of the object shape, mass, center of gravity and the number of robots involved. Similar centralized multi-robot coordination for object carrying were also later studied in [12] and [13].

Transportation of heavy objects using log rollers has a long history from the early civilizations [14]. However, no previous work to the best of our knowledge has studied object transportation using actuated rollers utilizing relative motion in the multi-robot arena. A grid-based cyclic multi-robot allocation and coordination method is proposed in this paper as preliminary work on implementing spherical robots for object carrying. Cyclic multi-robot coordination was previously proposed in [15] inspired by Emperor Penguin huddling in the Antarctic.

In this context, we emphasize the significance of GCRA proposed in this paper in Section IV, that it does not require further computation or adjustments in robot allocation for carrying once the initial cyclic grid system is initialized. The proposed grid generation method allows planar omnidirectional translation as shown under grid analysis with proof of stability in Section IV-C.

### III. PROBLEM STATEMENT

We define the object to be transported as an arbitrary planar shape  $C$  consisting of the set of  $m$  boundary points,

$$q_p = (x_p, y_p) \in \mathbb{R}^2, \quad p \in \{1, 2, \dots, m\} \quad (1)$$

relative to a global coordinate frame  $x^g y^g$ . The center-of-mass of the object is assumed to align with the geometric center of the shape and is denoted as  $q_c = (x_c, y_c)$  such that  $q_c \notin C$ .

A local coordinate frame  $x^b y^b$  is attached on the object at  $q_c$  with the object orientation relative to  $x^g y^g$  denoted as  $\theta$ .

$N$  robots are allocated on a grid formation relative to  $x^b y^b$  with spacing along the  $x$  and  $y$  axis defined as  $g_x$  and  $g_y$ . At any given time, allocated robots can be in either set A or set B; set A represent the robots under the planar shape  $C$ , and set B represent the robots around the object not directly involved in carrying.

We assume that  $C$  translates with a constant velocity  $v_0$ . The robots allocated under  $C$  form a convex hull defined as  $R$ . The rotation of the spherical robots under the defined shape  $C$  for object translation, results in relative velocity of the object to be twice the velocity of each of the spherical robots assuming no slip. Therefore, the relative velocity of  $R$  is half of  $C$ .

As robots on the trailing edge of  $R$  lose contact with  $C$ , more robots are required to be added on the leading edge to prevent the object from falling. We define the stability criterion of object carrying using spherical robots as follows.

*Definition 1: Object  $C$  of uniform weight distribution being carried by  $N$  spherical robots forming a convex hull  $R$  is stable, if the geometric centroid  $q_c$  of object  $C$  is always bounded within the convex hull  $R$ .*

The objective is to determine the grid spacing parameters  $g_x$  and  $g_y$  for the grid formation, and the minimum number of robots required denoted as  $N_{min}$ , such that stable transportation of the object defined as planar shape  $C$  is achieved based on the stability criterion defined in *Definition 1*.

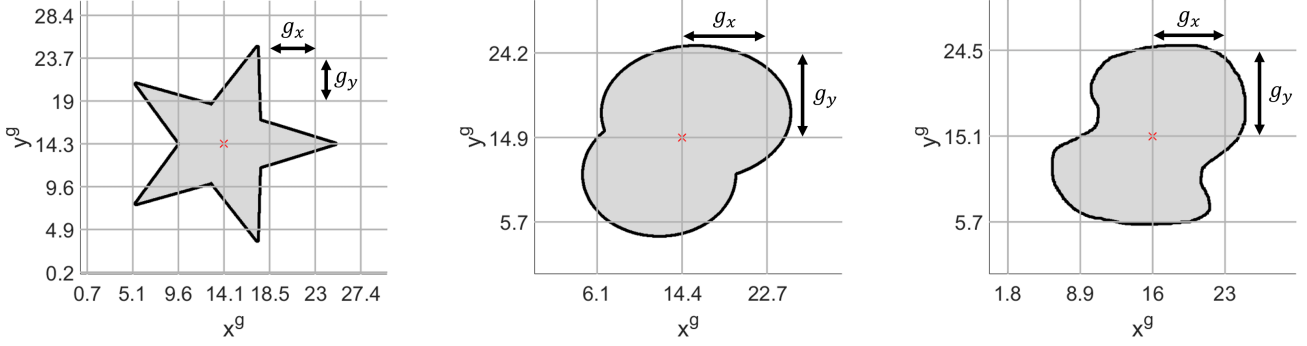
### IV. PROPOSED SOLUTION

We design the proposed GCRA method for spherical robots for object carrying, by defining the unit grid size parameters  $g_x$  and  $g_y$ , where the resulting grid intersections under  $C$  denote allocated robots.

#### A. Grid generation system

The horizontal grid spacing  $g_x$  relative to the local frame  $x^b y^b$  must be less than the minimum distance between the centroid  $q_c$  and  $q_p \in C$ ,  $\forall p \in \{1, 2, \dots, m\}$  for planar omnidirectional object translation. The set of lengths from  $q_c$  to  $q_p \in C$ ,  $\forall p \in \{1, 2, \dots, m\}$  along the  $x$ -axis for orientation  $\theta$  is calculated as,

$$\Delta x_\theta = \{|x_c - x_p| \mid y_p = y_c, \forall (x_p, y_p) \in C\}. \quad (2)$$



(a) Case 1: Generated grid for  $q_c = (14.1, 14.3)$  of star shape [ $g_x = 4.5, g_y = 4.7$ ]. (b) Case 2: Generated grid for  $q_c = (14.4, 14.9)$  of [ $g_x = 8.3, g_y = 9.3$ ]. (c) Case 3: Generated grid for  $q_c = (16, 15.1)$  of [ $g_x = 7.1, g_y = 9.4$ ].

Fig. 3: Grid generation with design parameters  $g_x$  and  $g_y$  for each of the validation cases C1: star shape, C2: arbitrary shape 1 and C3: arbitrary shape 2.

The horizontal grid spacing  $g_{x,\theta}$  is derived as,

$$g_{x,\theta} \leq \min(\Delta x_\theta). \quad (3)$$

To determine the minimum vertical grid spacing at orientation  $\theta$ , defined as  $g_{y,\theta}$ , we calculate the set of horizontal lengths of  $C$  as,

$$d_{pj,\theta} = \{|x_p - x_j| | y_p = y_j, \forall (x_p, y_j) \in C\}. \quad (4)$$

The set of lengths from  $q_c$  to  $q_p \in C$ ,  $\forall p = \{1, 2, \dots, m\}$  along the  $y$ -axis and equal to elements in  $d_{pj,\theta}$  for orientation  $\theta$  is calculated as,

$$\Delta y_\theta = \{|y_c - y_p| | (d_k = |x_p - x_j| | y_p = y_j), \forall (x_p, y_j) \in C\} \quad (5)$$

where  $d_k \in d_{pj,\theta}$ . Similarly, the vertical grid spacing  $g_{y,\theta}$  is defined as less than or equal to the minimum value of the set defined in Eq. (5) and written as,

$$g_{y,\theta} \leq \min(\Delta y_\theta). \quad (6)$$

The process is repeated to obtain the set of  $g_{x,\theta}$  and  $g_{y,\theta}$  for  $0 \leq \theta < \pi$  denoted as  $G_x$  and  $G_y$  respectively. The minimum grid size parameters  $g_x$  and  $g_y$  are determined as the minimum of its respective set.

We assume that the transport process is slow enough such that no slip occurs between each robot and the object surface. However, in reality we add an additional safety margin to  $g_x$  and  $g_y$  to account for movement inertia of  $C$  and any slip that may occur during the transport process as,

$$G_x = \{g_{x,\theta}\}, G_y = \{g_{y,\theta}\}, \text{ for } 0 \leq \theta < \pi \quad (7)$$

$$g_x = \min(G_x) - \delta x, g_y = \min(G_y) - \delta y \quad (8)$$

where  $\delta x$  and  $\delta y$  represent safety margins on the grid spacing design such that  $g_x > \delta x \geq 0$  and  $g_y > \delta y \geq 0$ . The grid generation process is illustrated in Fig. 2a, 2b and 2c.

### B. Robot Allocation

The grid intersections under  $C$  represent the allocated robots in set  $A$ . As the relative velocity of  $C$  is twice that of robots in  $A$ , a layer of robots is also required on the planar

movement direction to receive  $C$  as the object translates. Therefore, a layer of robots is also allocated around  $C$ .

*Definition 2:* At any given time all robots in  $A$  must have eight neighboring robots; two along  $\pm g_x$ , two along  $\pm g_y$  and four at  $\pm g_x$  and  $\pm g_y$  diagonal locations from its current position on the grid. The layer of robots fulfilling this requirement and not in set  $A$  allows omni-directional translation of  $C$  and constitutes robots of set  $B$ .

As  $C$  translates, robots in  $B$  on the trailing edge that do not fulfill *Definition 2*, are re-allocated continuously around  $C$  to fulfill *Definition 2*. Therefore, the minimum number of robots required for stable omni-directional transport of  $C$  is defined as  $N_{min} = |A \cup B|$ . Fig. 2d illustrates robot allocation based on the set  $A$  or set  $B$  classification.

We identify robot dynamics and control law for self-organizing to follow *Definition 2* as beyond the scope of the paper, but we conclude that a decentralized approach may be employed because of the cyclic nature of the proposed robot allocation method. At this stage, we focus on the robot allocation problem that ensures stable object transportation following *Definition 1*.

### C. Stability Analysis

In this section, we analytically investigate the stability of the proposed grid spacing design in transporting the planar shape  $C$  following the stability criterion presented in *Definition 1*.

*Proposition:* At any orientation  $\theta$  of  $C$ , the minimum horizontal distance from  $q_c$  to  $q_p \in C$ ,  $\forall p = \{1, 2, \dots, m\}$  along the  $x^+$  and along the  $x^-$  axis denoted as  $bg_x$  and  $ag_x$  respectively such that  $a + b = \alpha$ ,  $q_c$  is always bounded within  $R$ , if  $a \geq 0$  and  $b \geq 0$ .

*Proof:* The above setup yields the following conditions for stable object transportation along the  $x$ -axis:

$$(x_c + (\alpha - a)g_x) - x_c \geq 0, \quad (9)$$

$$x_c - (x_c - ag_x) \geq 0. \quad (10)$$

Based on our initial setup assumption that  $q_c \notin C$  and  $\delta x \geq 0$ , the grid spacing parameter  $g_x$  is always  $\mathbb{R}_{>0}$ . Therefore, following Eq. (9) we conclude that  $\alpha \geq a$ . Similarly, Eq. (10)

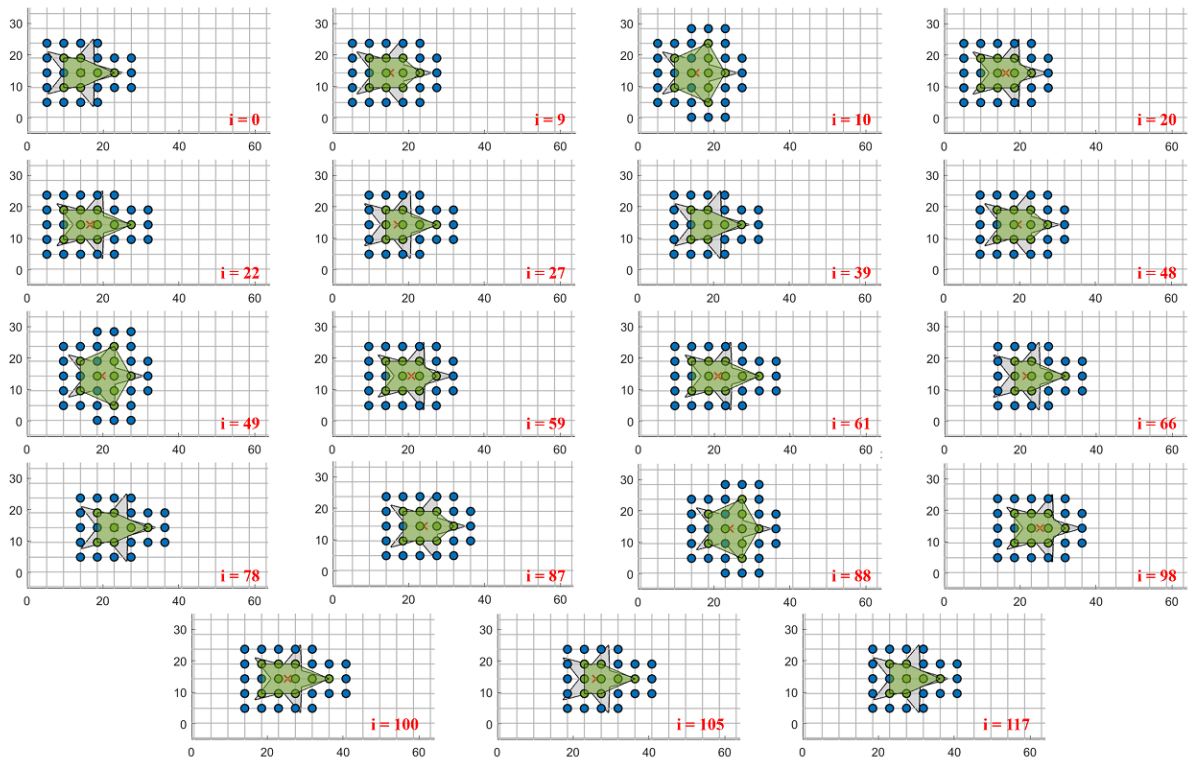


Fig. 4: Case 1: Star shape showing cycle time  $i = 39$  iterations. Simulation time lapse of 3 cycles of robot allocation showing changing hull  $R$  with  $v_0 = 0.065 \text{ x-units/iteration}$  and hull repetition.

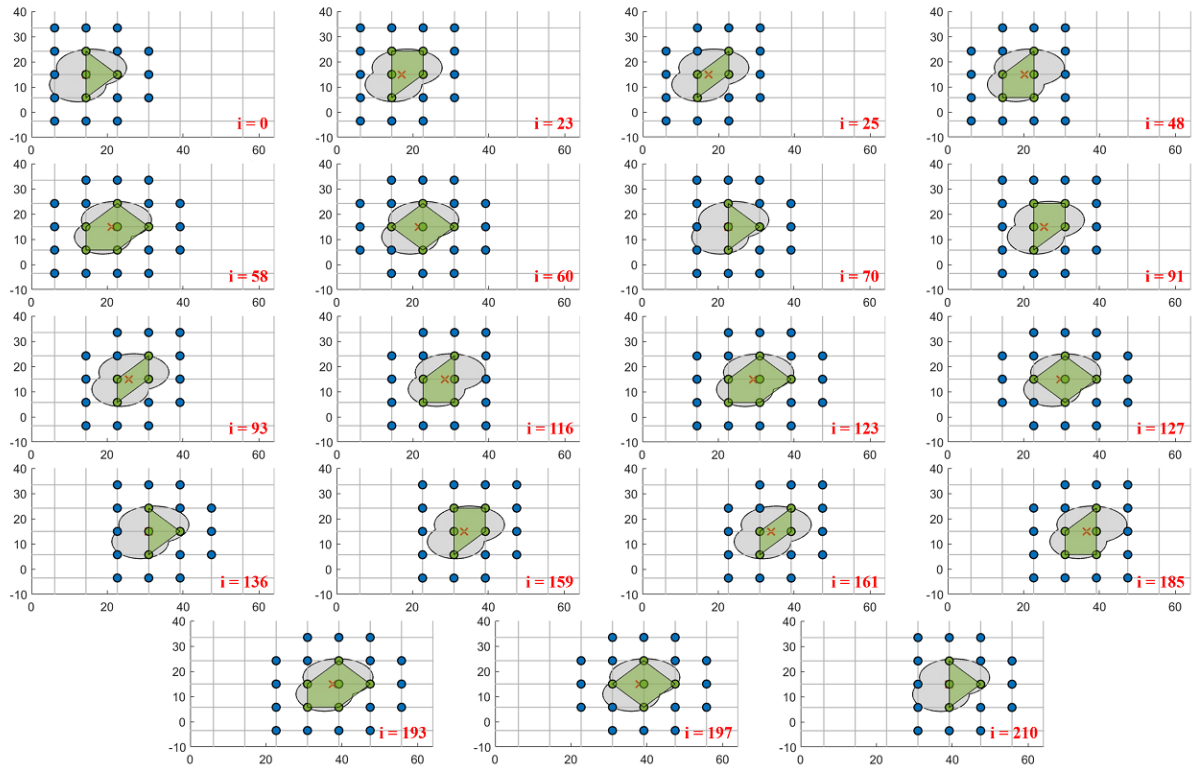


Fig. 5: Case 2: Arbitrary shape 1 showing cycle time  $i = 70$  iterations. Simulation time lapse of 3 cycles of robot allocation showing changing hull  $R$  with  $v_0 = 0.065 \text{ x-units/iteration}$  and hull repetition.

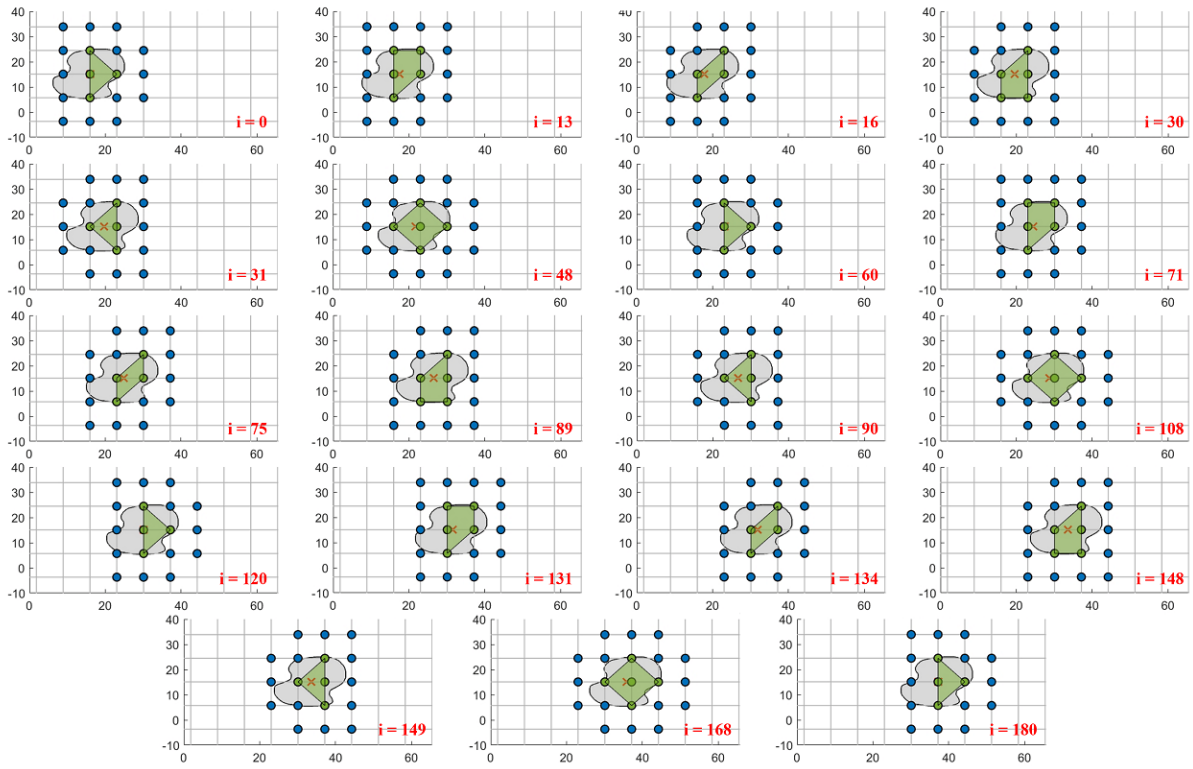


Fig. 6: Case 3: Arbitrary shape 2 showing cycle time  $i = 60$  iterations. Simulation time lapse of 3 cycles of robot allocation showing changing hull  $R$  with  $v_0 = 0.065$   $x$  -  $units/iteration$  and hull repetition.

TABLE I: Grid spacing parameters for validation cases

Case	$g_x$	$g_y$	$N_{min}$
C1: Star shape	7.1	5.2	34
C2: Arbitrary shape 1	8.3	9.3	22
C3: Arbitrary shape 2	7.1	9.4	21

suggests  $a \geq 0$  and hence,  $\alpha \geq 0$ . With  $\alpha \geq 0$  and  $a \geq 0$ , we conclude that  $b \geq 0$ . ■

The grid spacing parameter  $g_y$  is calculated based on  $g_x$  following Eq. (4) and (5). The stability of translation along the  $y$ -axis can be validated in a similar fashion. Since  $g_x$  and  $g_y$  are calculated based on the minimum distance to  $C$  from  $q_c$  for  $0 \leq \theta < 2\pi$ , the above proof holds true for omnidirectional planar translation.

## V. VALIDATION

### A. Setup

To validate our proposed concept of grid-based robot allocation for carrying objects using spherical robots, we consider cases of a star shape (C1) and two arbitrary shapes (C2 and C3) for object transportation. The objects are represented with high resolution boundary points in  $C$  and known centroids  $q_c$  for each case. Using the proposed grid generation method, the grid parameters  $g_x$  and  $g_y$  are calculated and the intersections of the grids are assumed to host spherical robots either under set  $A$  or set  $B$  for each of the cases C1, C2 and C3. Fig. 3 illustrates the cases and their generated grid based on spacing  $g_x$  and  $g_y$ .

We assume that for each of the cases, the object translates at a constant velocity  $v_0 = 0.065$   $x$  -  $units/iteration$ , slow

enough such that no slipping occurs at the contact areas between each robot and the object. Since the object dynamics and inertia are not considered at this stage, the grid parameters  $g_x$  and  $g_y$  are calculated with  $\delta x = 0$  and  $\delta y = 0$  safety margins for the presented simulations.

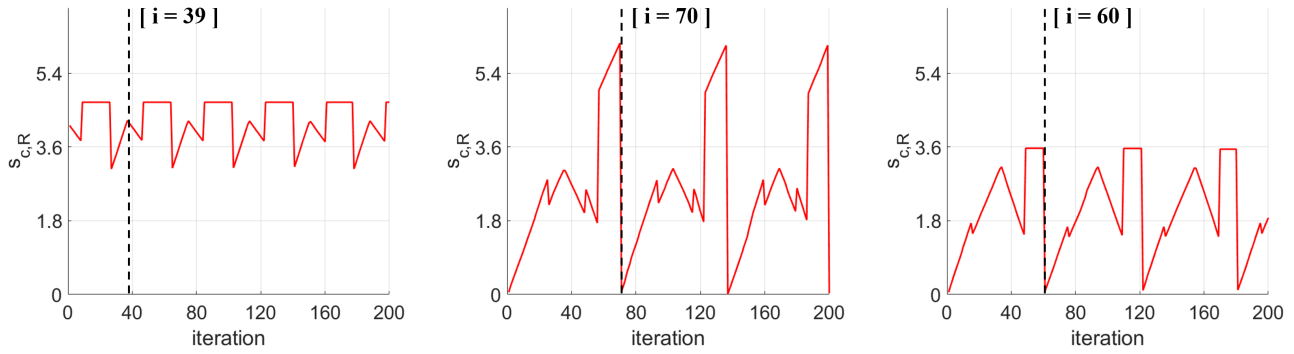
For validation purposes, the minimum distance from  $q_c$  to  $q_p \in C$ ,  $\forall p = \{1, 2, \dots, m\}$  denoted as  $s_{c,R}$  is measured at every iteration instance for each of the C1, C2 and C3 cases.

### B. Experiment and Results

Figure 4, 5 and 6 each illustrate the sequence of simulation time steps for each of the object cases C1, C2 and C3, for 3 cycles of GCRA based on the proposed grid generation method in this paper. In each of the cases, green robots represent set  $A$  forming the convex hull  $R$ , and blue robots represent set  $B$ . Table I shows the calculated grid spacing parameters and the minimum number of robots required for each of the simulation cases.

GCRA repeats every grid translation of the center  $q_c$  for each of the object cases. The set of convex hull  $R$  formations at every iteration during each cycle repeats over time forming a cyclic pattern in the measured  $s_{c,R}$  for each of the cases.

In case C1, the robot allocation pattern repeats every  $i = 39$  iterations. Iteration  $i = 10$  illustrates the allocation of the minimum number of robots required for safe transportation of the shape in a complete cycle as  $N_{min} = 34$ . Similarly in cases C2 and C3, the robot allocation process repeats every  $i = 70$  and  $i = 60$  iterations, with the allocation of the minimum number of robots required for safe transportation



(a) Case 1: Shortest distance between centroid  $q_c$  to boundary of the convex hull  $R$ . [Cycle duration,  $i = 39$ ]  
 (b) Case 2: Shortest distance between centroid  $q_c$  to boundary of the convex hull  $R$ . [cycle duration,  $i = 70$ ]  
 (c) Case 3: Shortest distance between centroid  $q_c$  to boundary of the convex hull  $R$ . [Cycle duration,  $i = 60$ ]

Fig. 7: Plot showing the shortest distance between  $q_c$  to boundary of the convex hull  $R$  during the transportation process.

of each shape in a complete cycle  $N_{min} = 22$  and  $N_{min} = 21$  illustrated at  $i = 58$  and  $i = 48$  iterations respectively.

Figure 7a, 7b and 7c plot measured  $s_{c,R}$  for each of the object transportation cases C1, C2 and C3 with iteration. In each of the cases,  $s_{c,R}$  remains greater than or equal to zero throughout each repeating cycle validating the proposed  $g_x$  and  $g_y$  based grid generation method. The simulations for each case were performed with safety margins of  $\delta x = 0$  and  $\delta y = 0$ . The increment of the safety margins will decrease the grid spacing parameters  $g_x$  and  $g_y$ . This will increase minimum  $s_{c,R}$  of case C1, C2 and C3 during the transportation process.

A video of the simulations is available for reference at <http://smart-laboratory.org/docs/obj.mp4>.

## VI. CONCLUSION AND FUTURE WORK

In this paper, a grid-based cyclic robot allocation method for object carrying by spherical robots is proposed. Problems of grid size parameter design and the minimum number of robots required based on arbitrary object shape are addressed such that stable omni-directional object translation can be achieved. Due to the cyclic nature of the robot allocation method, a decentralized approach to multi-robot control may be implemented. Stability of object carrying with the proposed robot allocation methodology is analytically proven. Simulation results validate the proposed concept illustrating the object centroid always bounded by the convex hull of the allocated carrying robots. The proposed object carrying method using a multi-robot system of spherical robots requires further investigation on cost and feasibility analysis depending on robot design. However, referring to the long history of successful object transportation by log rollers, we believe it is a viable alternative to the current methods of grasping, pushing or caging.

With successful robot allocation, further work on developing multi-robot self-organizing control laws to accommodate the required robot allocation positions in a cyclic manner for omni-directional translation along with experimental validation is underway.

## REFERENCES

- [1] J. Alonso-Mora, S. Baker, and D. Rus, "Multi-robot formation control and object transport in dynamic environments via constrained optimization," *The International Journal of Robotics Research*, vol. 36, no. 9, pp. 1000–1021, 2017.
- [2] J. Chen, M. Gauci, and R. Groß, "A strategy for transporting tall objects with a swarm of miniature mobile robots," in *2013 IEEE International Conference on Robotics and Automation*. IEEE, 2013, pp. 863–869.
- [3] W. Wan, B. Shi, Z. Wang, and R. Fukui, "Multirobot object transport via robust caging," *IEEE transactions on systems, man, and cybernetics: systems*, no. 99, pp. 1–11, 2017.
- [4] V. A. Joshi, R. N. Banavar, and R. Hippalgaonkar, "Design and analysis of a spherical mobile robot," *Mechanism and Machine Theory*, vol. 45, no. 2, pp. 130–136, 2010.
- [5] V. Kaznov, F. Bruhn, P. Samuelsson, and L. Stenmark, "Ball robot," Jan. 17 2012, uS Patent 8,099,189.
- [6] E. Tuci, M. H. Alkilabi, and O. Akanyeti, "Cooperative object transport in multi-robot systems: A review of the state-of-the-art," *Frontiers in Robotics and AI*, vol. 5, p. 59, 2018.
- [7] D. J. Stilwell and J. S. Bay, "Toward the development of a material transport system using swarms of ant-like robots," in *[1993] Proceedings IEEE International Conference on Robotics and Automation*. IEEE, 1993, pp. 766–771.
- [8] P. J. Johnson and J. S. Bay, "Distributed control of simulated autonomous mobile robot collectives in payload transportation," *Autonomous Robots*, vol. 2, no. 1, pp. 43–63, 1995.
- [9] G. A. Pereira, B. S. Pimentel, L. Chaimowicz, and M. F. Campos, "Coordination of multiple mobile robots in an object carrying task using implicit communication," in *Proceedings 2002 IEEE International Conference on Robotics and Automation (Cat. No. 02CH37292)*, vol. 1. IEEE, 2002, pp. 281–286.
- [10] C. C. Loh and A. Traechtler, "Cooperative transportation of aload using nonholonomic mobile robots," *Procedia Engineering*, vol. 41, pp. 860–866, 2012.
- [11] B. Hichri, L. Adouane, J.-C. Fauroux, Y. Mezouar, and I. Doroftei, "Cooperative mobile robot control architecture for lifting and transportation of any shape payload," in *Distributed Autonomous Robotic Systems*. Springer, 2016, pp. 177–191.
- [12] Z.-D. Wang, E. Nakano, and T. Matsukawa, "Cooperating multiple behavior-based robots for object manipulation," in *Distributed Autonomous Robotic Systems*. Springer, 1994, pp. 371–382.
- [13] A. Yamashita, T. Arai, J. Ota, and H. Asama, "Motion planning of multiple mobile robots for cooperative manipulation and transportation," *IEEE Transactions on Robotics and Automation*, vol. 19, no. 2, pp. 223–237, 2003.
- [14] J. Li and H. Chen, "Lubrication for transporting heavy objects in the history," *Tribology Online*, vol. 11, no. 2, pp. 242–248, 2016.
- [15] T. Mina and B.-C. Min, "Penguin huddling-inspired energy sharing and formation movement in multi-robot systems," in *2018 IEEE International Symposium on Safety, Security, and Rescue Robotics (SSRR)*. IEEE, 2018, pp. 1–8.